Multiphase Load-flow Solution of Induction Machines

I. Kocar, *Senior Member, IEEE*, U. Karaagac, *Member, IEEE*, J. Mahseredjian, *Fellow, IEEE,* B. Cetindag, *Student Member*

***Abstract*—This paper presents a new method to model induction machines (IMs) in multiphase load-flow calculations. Fast convergence of the load-flow solution is achieved using an iterative Newton method in the modified-augmented-nodal-analysis (MANA) formulation. The multiphase modeling approach allows accounting for unbalanced networks. The IM is modeled using either a constraint of electrical power input, mechanical power or mechanical torque output. The slip of the IM becomes a load flow variable computed iteratively while the reactive power is not fixed. In addition, the initialization of time domain simulations using load flow solution in the computation of electromagnetic transients is demonstrated using balanced and unbalanced network cases. It is shown that a seamless transition between load-flow and time-domain average powers is obtained when the slip of the IM is formulated as a variable in load flow and its reactive power is not fixed.**

***Index Terms*— Induction Machine, EMTP, Initialization from Load-Flow, Distribution Systems, Multiphase Load-Flow**

I. Introduction

THE initialization of the time-domain solution in the computation of electromagnetic transients, requires using a multiphase unbalanced load-flow solution followed by a steady-state solution with equivalent models transposed into time-domain. The multiphase load-flow solvers are capable of handling distributed generation units [1]-[5] with generalization for arbitrary devices and network topologies [6]. The asynchronous induction machines (IM), are often modeled as constant PQ devices in the load-flow solution, but there is no direct relation between real and reactive powers of the IM and this approach cannot provide sufficiently accurate initialization for the time-domain solution. Another approach to model the IM has been to use a constant slip [7]. In this case, the IM is modeled as a shunt branch. Although this approach can yield better results, it is often not possible to specify a sufficiently accurate slip value.

An initial test case is developed by the Distribution System Analysis Subcommittee [8] for the validation of IM models under unbalanced conditions in three phase distribution system analysis software. The machine in this test case is specified with input electrical power and the model must compute the slip and reactive power. An IM model that can handle input electrical power constraint is presented in [9]. This method is developed for fixed-point load-flow solvers, such as the backward forward sweep solvers [10]-[18], and requires an additional iterative loop or nonlinear solution for IMs after each load-flow iteration for the determination of slip using the voltage conditions and input electrical power constraint. The solution gets more demanding when there are several machines in the network. It is also known that fixed-point methods have poor convergence properties.

This paper proposes a new method to model IMs in unbalanced load-flow calculations. The new method is based on the modified-augmented-nodal-analysis (MANA) formulation using the iterative Newton's method. The new method can be used for single and double cage IMs. It allows modeling the IM with electrical power input, mechanical power or mechanical torque output. The slip of the IM becomes a load-flow variable computed iteratively. The reactive power is a function of real power constraint and slip or voltage solution of the IM, therefore it is not fixed. The proposed solution reduces the number of iterations radically as compared to fixed-point solution methods. The presented generic formulation is not currently available in the literature.

The method presented in this paper is developed using the modified-augmented-nodal-analysis (MANA) formulation [19]-[20]. The MANA formulation establishes a generic multiphase load-flow formulation framework that can handle arbitrary network topologies, and can be easily and systematically extended to accommodate various component models [6].

The load-flow solution promulgated in this paper allows accurate initialization of time-domain simulations of electromagnetic transients (EMTs). An EMT solver [19] is used to demonstrate that the time-domain simulations of practical networks with IMs can be accurately initialized if the reactive power is not fixed and the slip is computed as a variable in the load-flow solution. The proposed load-flow method and EMT combination for initialization of time-domain simulations, is an important contribution in this paper.

This paper presents first the load-flow solver then contributes the inclusion of IM equations. The examples and comparisons demonstrate the advantages of the proposed solution both in steady-state and time-domain studies.

Ilhan Kocar, Baki Cetindag and Jean Mahseredjian are with Polytechnique Montréal, QC. Ulas Karaagac is with Hong Kong Polytechnic University. (ilhan.kocar@polymtl.ca, baki.cetindag@polymtl.ca, ukaraa@polyu.edu.hk, jean.mahseredjian@polymtl.ca)

II. Background

A. MANA Formulation

It is helpful first to briefly recall the MANA formulation [19], [20] and cite related literature for readers willing to investigate the basis on which the proposed technique is built. The MANA formulation of network equations is obtained by simply augmenting the classical nodal equations with supplementary component equations. This results into a generic system of equations.

$$\mathbf{Ax} = \mathbf{b} \tag{1}$$

In this paper bold characters are used for matrices and vectors. In the above steady-state equation, $\mathbf{A}$ is the system (coefficient) matrix, $\mathbf{x}$ is the vector of unknowns and $\mathbf{b}$ is the vector of known variables. An expanded view of the same system is given by

$$\begin{bmatrix} \mathbf{Y_n} & \mathbf{A_c} \\ \mathbf{A_r} & \mathbf{A_d} \end{bmatrix} \begin{bmatrix} \mathbf{V_n} \\ \mathbf{I_x} \end{bmatrix} = \begin{bmatrix} \mathbf{I_n} \\ \mathbf{V_x} \end{bmatrix} \tag{2}$$

where $\mathbf{Y_n}$ is the classical multiphase nodal admittance matrix; the matrices $\mathbf{A_r}$, $\mathbf{A_c}$ and $\mathbf{A_d}$ (augmented portion, row, column and diagonal coefficients) are used to enter (interface with) network model equations which are not or cannot be included in $\mathbf{Y_n}$; $\mathbf{V_n}$ and $\mathbf{I_x}$ are the vectors of unknown node voltages and component currents respectively; $\mathbf{I_n}$ and $\mathbf{V_x}$ are the vectors of known nodal currents and component voltages respectively. In a more generic version it is possible to use other network variables instead of currents $\mathbf{I_x}$ and voltages $\mathbf{V_x}$. Further partitioning of the matrices is shown in [19] and [20] for illustration purposes, but in reality, component equations can be entered in any order and the partitioning of (2) is also used for explanation purposes. Simple examples and application of MANA to distribution system steady-state analysis have been provided in [21]. The MANA formulation is also used for multiphase state estimation of distribution networks by incorporating it with Hachtel's formulation [22].

B. MANA Load-Flow Method

It is recalled that for a generic matrix function $\mathbf{f(x)} = \mathbf{0}$, the Newton method is used to write

$$\mathbf{f}(\mathbf{x}^{(j)}) + \mathbf{J}^{(j)}\Delta\mathbf{x}^{(j)} = 0 \tag{3}$$

$$\mathbf{x}^{(j+1)} = \mathbf{x}^{(j)} + \Delta\mathbf{x}^{(j)} \tag{4}$$

where j is the iteration counter, $\mathbf{x}$ is the vector of the unknowns, $\mathbf{J}$ is the Jacobian matrix and $\Delta\mathbf{x}$ is the correction vector.

The MANA approach can be used to construct the Jacobian matrix as explained in detail in [6]. It is sufficient to augment (2) with load-flow constraints from various devices. The resulting generic system of equations with the introduction of IM constraints developed in this paper is given by

$$\begin{bmatrix} \mathbf{Y_n} & \mathbf{A_c} & \mathbf{A_{IL}} & \mathbf{A_{IG}} & \mathbf{0} & \mathbf{A_{IM}} \\ \mathbf{A_r} & \mathbf{A_d} & \mathbf{0} & \mathbf{0} & \mathbf{0} & \mathbf{0} \\ \mathbf{J_L} & \mathbf{0} & \mathbf{J_{LI}} & \mathbf{0} & \mathbf{0} & \mathbf{0} \\ \mathbf{Y_G} & \mathbf{0} & \mathbf{0} & \mathbf{B_{GI}} & \mathbf{B_{GE}} & \mathbf{0} \\ \mathbf{J_{GPQ}} & \mathbf{0} & \mathbf{0} & \mathbf{J_{GPQI}} & \mathbf{0} & \mathbf{0} \\ \mathbf{J_{GPV}} & \mathbf{0} & \mathbf{0} & \mathbf{0} & \mathbf{0} & \mathbf{0} \\ \mathbf{J_{GSL}} & \mathbf{0} & \mathbf{0} & \mathbf{0} & \mathbf{0} & \mathbf{0} \\ \mathbf{J_{IMV}} & \mathbf{0} & \mathbf{0} & \mathbf{0} & \mathbf{0} & \mathbf{J_{IMS}} \end{bmatrix}^{(j)} \begin{bmatrix} \Delta\mathbf{V_n} \\ \Delta\mathbf{I_x} \\ \Delta\mathbf{I_L} \\ \Delta\mathbf{I_G} \\ \Delta\mathbf{E_G} \\ \Delta\mathbf{s_{IM}} \end{bmatrix} = - \begin{bmatrix} \mathbf{f_n} \\ \mathbf{f_x} \\ \mathbf{f_L} \\ \mathbf{f_{GI}} \\ \mathbf{f_{GPQ}} \\ \mathbf{f_{GPV}} \\ \mathbf{f_{GSL}} \\ \mathbf{f_{IM}} \end{bmatrix}^{(j)} \tag{5}$$

The sub-matrices $\mathbf{A_{IL}}$ and $\mathbf{A_{IG}}$ are adjacency matrices for interfacing the load ($\mathbf{I_L}$) and generator ($\mathbf{I_G}$) currents with the corresponding passive network nodes. The following sub-matrices are used to include load-flow constraints for any number of phases: $\mathbf{J_L}$ and $\mathbf{J_{LI}}$ for PQ-loads; $\mathbf{Y_G}$, $\mathbf{B_{GI}}$ and $\mathbf{B_{GE}}$ for generator current equations; $\mathbf{J_{GPQ}}$ and $\mathbf{J_{GPQI}}$ for PQ-type generators; $\mathbf{J_{GPV}}$ for PV-type generators; $\mathbf{J_{GSL}}$ for slack-type generators (buses); $\mathbf{J_{IMV}}$ and $\mathbf{J_{IMS}}$ for IMs. The unknown supplementary vectors are defined as follows: $\mathbf{I_L}$ is for PQ-load currents, $\mathbf{I_G}$ is for generator currents, $\mathbf{E_G}$ represents generator internal voltages and $\mathbf{s_{IM}}$ is for the slips of IMs. $\mathbf{A_{IM}}$ is for interfacing IM slips with network nodes.

Equation (5) is a real system which means that each unknown has two parts (real and imaginary). This formulation is like the one presented in [6], except that it is extended with IM equations. The next section focuses on the integration of IM equations.

III. Formulation of the Induction Machine Equations for Power Flow Calculation

A. Equivalent Circuit Equations

It is useful to resort to sequence networks of an IM in order to develop load-flow equations. The Steinmetz equivalent circuit (see Fig. 1) is directly used as the positive sequence network. The negative sequence network differs only in the value of the slip, because it creates a rotating flux in an opposite direction, thus the negative slip s_n becomes

$$s_n = \frac{\omega_s + \omega_r}{\omega_s} = \frac{2\omega_s - (\omega_s - \omega_r)}{\omega_s} = 2 - s \tag{6}$$

$$s = \frac{\omega_s - \omega_r}{\omega_s} \tag{7}$$

where s is the (positive) slip, ω_s is the synchronous speed (rad/s) and ω_r is the rotational speed (rad/s).

Fig. 1 shows the equivalent circuit of a single cage IM. The positive and negative sequence networks are the same except for the value of slip. Since the IMs are typically connected in delta or ungrounded wye configuration, the zero sequence current is taken as zero.

The circuit parameters are written as a function of the slip and cage factor (*CF*) with the following definitions: r_s is stator resistance, x_s is stator reactance, r_m stands for core

losses, x_m is magnetizing reactance, $r_r'/s = r_r(1+CF_r\,s)/s$ is rotor resistance and $x_r' = x_r(1+CF_x\,s)$ is rotor reactance. The same approach can be applied to a double-cage IM.

The next step is to write the positive Z_1 and negative Z_2 sequence impedances at the terminals of the machine.

In the case of single cage IM (Fig. 1)

$$Z_1(s) = r_s + jx_s + \frac{1}{\frac{1}{k_1} + \frac{1}{r_m} - \frac{j}{x_m}} \tag{8}$$

where

$$k_1 = \frac{r_r(CF_r\ s+1)}{s} + jx_r(CF_x\ s+1) \tag{9}$$

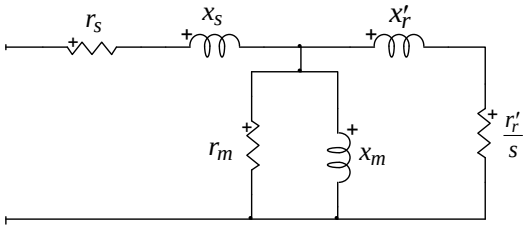

Fig. 1 Sequence network for single cage induction machine

For the negative sequence impedance Z_2 at the terminals of the negative sequence network

$$Z_2(s) = r_s + jx_s + \frac{1}{\frac{1}{k_4} + \frac{1}{r_m} - \frac{j}{x_m}} \tag{10}$$

where

$$k_4 = \frac{r_r\left[CF_r\ (2-s)+1\right]}{(2-s)} + jx_r\left[CF_x\ (2-s)+1\right] \tag{11}$$

By using the parameters found from the equivalent circuits, the terminal voltages and currents are written as

$$\mathbf{I_{abc}} = \mathbf{Y_{abc}V_{abc}} = \mathbf{AY_{012}A^{-1}V_{abc}} \tag{12}$$

$$\mathbf{I_{012}} = \mathbf{Y_{012}V_{012}} \tag{13}$$

where $\mathbf{A}$ is the Fortescue's transformation matrix, the subscript abc is used to denote phase domain terminal voltages ($\mathbf{V_{abc}}$) and currents ($\mathbf{I_{abc}}$), the subscript 012 denotes sequence domain voltages ($\mathbf{V_{012}}$) and currents ($\mathbf{I_{012}}$), and the admittance matrix is a function of slip *s*:

$$\mathbf{Y_{012}}(s) = \begin{bmatrix} 0 & 0 & 0 \\ 0 & Y_1(s) & 0 \\ 0 & 0 & Y_2(s) \end{bmatrix} \tag{14}$$

where $Y_1 = G_1 + jB_1 = 1/Z_1$ and $Y_2 = G_2 + jB_2 = 1/Z_2$ need to be updated at each iteration using the new slip value.

B. Power and Torque Relations for an Induction Machine

The total electrical power input of an IM is found by the formula

$$S_{in} = \mathbf{V_{abc}^t I_{abc}^*} = 3\left(V_0 I_0^* + V_1 I_1^* + V_2 I_2^*\right) \tag{15}$$

where the sign * indicates the complex-conjugate operator. The electrical power input is found from (15):

$$P_{in} = 3|V_1|^2\ G_1 + 3|V_2|^2\ G_2 = 3\left(P_1 + P_2\right) \tag{16}$$

In (16) the total power input has two sequence components one positive (P_1) and one negative (P_2). The air-gap powers for the two sequences are found by subtracting the stator loss from the input power.

$$P_{g1} = P_1 - r_s\,|I_1|^2 \tag{17}$$

$$P_{g2} = P_2 - r_s\,|I_2|^2 \tag{18}$$

where I_1 and I_2 are positive and negative sequence currents respectively. The available mechanical powers for positive and negative sequences are given by

$$P_{d1} = \left(1-s\right)P_{g1} \tag{19}$$

$$P_{d2} = \left(1-s_n\right)P_{g2} \tag{20}$$

The total mechanical power is found by combining (6), (19), (20), (17) and (18):

$$\begin{aligned} P_{mech} &= 3\left(P_{d1} + P_{d2}\right) \\ &= 3\left(1-s\right)\left(|V_1|^2\ G_1 - r_1\,|I_1|^2 - |V_2|^2\ G_2 + r_1\,|I_2|^2\right) \end{aligned} \tag{21}$$

From the relation $P_{mech} = T_{mech}\omega_m$ between mechanical power in (21) and mechanical torque T_{mech}, it is possible to write

$$T_{mech} = 3\frac{n_p}{\omega_s}\left(|V_1|^2\ G_1 - r_1\,|I_1|^2 - |V_2|^2\ G_2 + r_1\,|I_2|^2\right) \tag{22}$$

where n_p is the number of pole-pairs and it is recalled that $\omega_m = \omega_s(1-s)/n_p$.

IV. Induction Machine Load-Flow Equations

The IM can be characterized with one of the following constraint types: electrical power input, mechanical power output or mechanical torque. The slip is an unknown variable. The equivalent circuit of the machine participates in the nodal admittance matrix $\mathbf{Y_n}$ of (5). The supplementary Jacobian terms can be systematically obtained by taking the partial derivatives of constraint functions with respect to load-flow variables.

A. Contributions to nodal admittance matrix

Let the i^{th} IM be connected to the k^{th} three-phase bus with $\mathbf{k} = \begin{bmatrix} k_1 & k_2 & k_3 \end{bmatrix}$ the vector of node numbers. The contributions to $\mathbf{Y_n}$ are written as

$$\mathbf{Y_{kk}} = \mathbf{Y'_{kk}} + \mathbf{Y^i_{IM}} \tag{23}$$

where $\mathbf{Y'_{kk}}$ is related existing network component admittances (all other components connected to this node), $\mathbf{Y^i_{IM}}$ is the terminal admittance matrix of the IM. It is calculated from the sequence admittances of the IM and updated at each iteration using the recent slip value (see (14)).

$$\mathbf{Y^i_{IM}} = \mathbf{AY^i_{012}A^{-1}} \tag{24}$$

Since the IM currents are related to voltages and slip, their contributions into the Jacobian matrix of (5) are into the coefficients of voltages with (24) and into the matrix $\mathbf{A_{IM}}$ for

the slip term $\Delta \mathbf{s_{IM}}$. For the i^{th} IM

$$\mathbf{A_{IM}}(\mathbf{k},i) = \left[\frac{\partial \mathbf{Y_{IM}^i}}{\partial s_i}\right]\mathbf{V_n}(\mathbf{k}) \tag{25}$$

where

$$\frac{\partial \mathbf{Y_{IM}^i}}{\partial s_i} = \mathbf{A}\begin{bmatrix} 0 & 0 & 0 \\ 0 & \frac{\partial Y_1^i}{\partial s_i} & 0 \\ 0 & 0 & \frac{\partial Y_2^i}{\partial s_i} \end{bmatrix}\mathbf{A}^{-1} \tag{26}$$

The symbolic forms of Y_1 and Y_2 are found from Z_1 and Z_2 derived in Section III (see also (14)).

B. Evaluation of supplementary Jacobian terms

The supplementary coefficients $\mathbf{J_{IMV}}$ and $\mathbf{J_{IMS}}$ depend on the type of constraint defined for the IM. The following derivations are straightforward, and a Jacobian matrix based solution is obtained with the inherent convergence and robustness advantages.

1) Condition 1: Electrical power input constraint

From (16) the i^{th} IM constraint function becomes

$$f_{IM} = P_{in} - 3\left(V_{1R}^2 + V_{1I}^2\right)G_1 + 3\left(V_{2R}^2 + V_{2I}^2\right)G_2 \tag{27}$$

where P_{in} is specified, the index i has been dropped to simplify notation, and the sequence voltages must be written with real (subscript R) and imaginary (subscript I) parts. The voltages V_{1R} , V_{1I} , V_{2R} and V_{2I} are related to phase domain voltages $\mathbf{V_n}(\mathbf{k})$ (real and imaginary parts) through Fortescue transformation. The terms G_1 and G_2 are functions of slip according to (14). Thus the differentiation of (27) will contribute to the submatrix $\mathbf{J_{IMV}}$ for real and imaginary voltages in $\Delta\mathbf{V_n}(\mathbf{k})$ and to the submatrix $\mathbf{J_{IMS}}$ for the slip s_i .

2) Condition 2: mechanical power output constraint

From equation (21) the constraint function is given by

$$f_{IM} = P_{mech} - 3(1-s)\left(|V_1|^2 G_1 - r_1 |I_1|^2 - |V_2|^2 G_2 + r_1 |I_2|^2\right) \tag{28}$$

where the mechanical power P_{mech} is specified. Once again differentiation is applied here and contributes to the coefficient matrices $\mathbf{J_{IMV}}$ and $\mathbf{J_{IMS}}$.

3) Condition 3: mechanical torque

From equation (22) the constraint function becomes

$$f_{IM} = T_{mech} - 3\frac{n_p}{\omega_s}\left(|V_1|^2 G_1 - r_1 |I_1|^2 - |V_2|^2 G_2 + r_1 |I_2|^2\right) \tag{29}$$

where the mechanical torque T_{mech} is the specified constraint and the differentiation of (29) contributes to $\mathbf{J_{IMV}}$ and $\mathbf{J_{IMS}}$.

C. Initialization

The initial parameters of the IM are obtained according to the IM constraint.

If the input electrical power is given, the reactive power of the IM is initially taken as the half of the real power

$$S_{IM} = P_{IM} + j(P_{IM}/2) \tag{30}$$

If the mechanical power output is the constraint, the input electrical power is approximated by taking into account the stator losses as follows

$$P_{IM} = P_{mech} + r_s \frac{\left|P_{mech} + jP_{mech}/2\right|^2}{\left|V_{line}\right|^2} \tag{31}$$

The total complex input power S_{IM} is then calculated using (30).

If the mechanical torque is given, the electrical power is computed as follows

$$P_{IM} = \frac{T_{mech}}{n_p}\omega_s \tag{32}$$

The input apparent power S_{IM} is again calculated using (30).

V. RESULTS

The solution method presented in this paper can be applied to both single and double cage IMs. The two cases used below are taken from IEEE test cases and for single cage IMs. The first case (Case-1) utilizes a test case specifically developed to validate IM models [8] for distribution system analysis. The second case (Case-2) is a modified version of the IEEE 34-BUS Test Feeder [23] and allows verifying performance and convergence stability characteristics of the technique proposed in this paper. In the following section the new solution method is tagged as "New Method" and referenced literature results are identified by "Published".

A. Case-1: Induction Machine Test Case

The aim of the 4-BUS test case in Fig. 2 is to provide a reference for developers to validate their models of IMs under unbalanced conditions, as stated in [8].

The machine ASM1 in Fig. 2 is a single cage IM connected to BUS2LV. The machine parameters are given in Table I.

In this test case, the IM is characterized with a "constant input electrical power" of 1000 kW (constraint Condition 1).

Using the load-flow method presented in this paper, the final slip of the IM has been found as 0.00727434. This is very close to the published result of 0.00727714. The published results are obtained using the fixed-point methodology as described in [25].

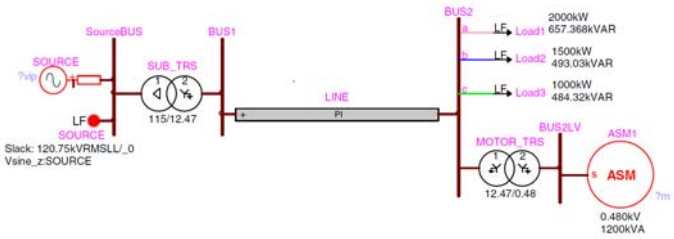

Fig. 2 Network schematic for induction machine test case (from [24]), Case-1

TABLE I MACHINE PARAMETERS, CASE-1

Rated Voltage	480 V
Rating	1200 kVA
Nominal Power	1000 kW
Stator Resistance	0.0053 pu
Stator Reactance	0.106 pu
Rotor Resistance	0.007 pu
Rotor Reactance	0.12 pu
Mag. Branch Reactance	4 pu

The total real and reactive powers delivered to the IM are 1000 kW and 490 kvar respectively.

Tables II-III compare the published results with those found in this paper. The number of iterations required to make Δs less than 1e-6, is only 3 with the proposed technique, while the fixed-point method of [9] requires 21 iterations. The reason that the proposed method requires less iterations is because it uses Newton's method, and the slips of the IMs are directly populated in the Jacobian matrix as variables.

The variation of slip versus iteration number is given in Fig. 3.

TABLE II COMPARISON OF SEQUENCE CURRENTS, CASE-1

	NEW METHOD	PUBLISHED
Sequence currents	**Magnitude (A)**	**Magnitude (A)**
I_1	1416.2	1416.6
I_2	80.4	80.6557

TABLE III VALIDATION OF NODE VOLTAGES, CASE-1

	NEW METHOD		PUBLISHED	
BUS	**Magnitude (V)**	**Angle (deg.)**	**Magnitude (V)**	**Angle (deg.)**
BUS1a	7324	-33.1	7323	-33.1
BUS1b	7386	-152.4	7385	-152.4
BUS1c	7402	88.3	7401	88.3
BUS2a	6810	-36.4	6809	-36.4
BUS2b	7230	-154.9	7229	-154.9
BUS2c	7201	87.7	7200	87.7
BUS2LVa	253	-39.2	253	-39.2
BUS2LVb	268	-157.8	268	-157.8
BUS2LVc	265	85.05	265	85.0

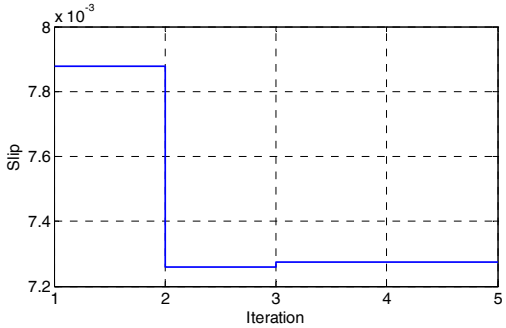

Fig. 3 Iteration vs. slip (3 iterations with a tolerance of ε<1e-6), Case-1

B. Case-2: IEEE 34-BUS Test Feeder

This network case is developed by the Distribution System Analysis Subcommittee of the Power Systems Analysis, Computing and Economics Committee [25]. In this test case, the original IEEE 34-BUS Test Feeder is modified by adding two IMs rated at 480 V, 660 kW together with their power transformers as shown in Fig. 4. The detailed model parameters can be found in [25]. Both IMs are in generator mode and modeled with constant electrical power generation constraint at their terminals (negative electrical input). This IEEE test case sets another validation for the proposed technique and allows comparing its convergence characteristics with the existing fixed point technique.

The proposed new load-flow method for IMs converges in 4 iterations as shown in Fig. 5, while it takes 28 iterations with the fixed-point method presented in [25] when the tap positions of regulators are fixed. The fixed-point method requires an external procedure to compute the slip of IMs using the updated terminal voltages after each load-flow iteration. If the IMs are modeled as simple PQ devices, then the fixed-point method converges in 15 iterations and the Newton method in 3 iterations.

The electrical parameters of the IMs are presented in Table IV for convenience. The final reactive powers, slip values and sequence currents are shown in Tables V and VI respectively. The two IMs are operated in generator mode; therefore, both the initial slips and the resultant slips are negative. Table VII demonstrates matching load-flow results for arbitrarily selected buses.

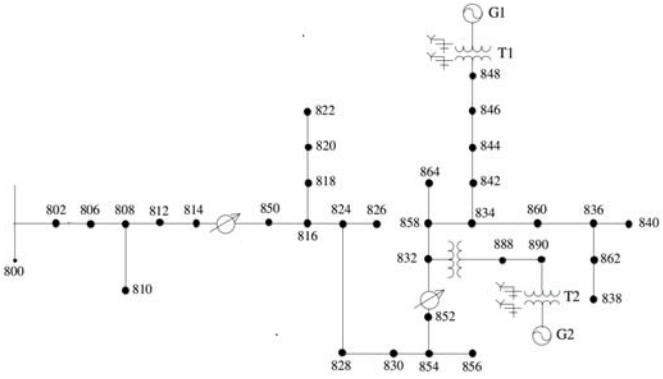

Fig. 4 One-line diagram of 34-bus test feeder system with two induction generators, G1 and G2, Case-2

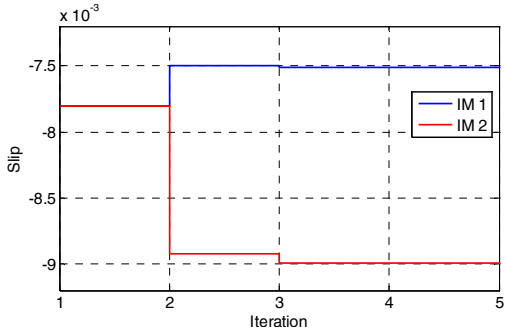

Fig. 5 Iteration vs. slip for the IEEE 34-BUS test system (4 iterations with a tolerance of ε<1e-6), Case-2

TABLE IV MACHINE PARAMETERS, CASE-2

Rated Voltage	480 V
Power Base	660 kVA
Nominal Power	660 kW
Stator Resistance	0.0053 pu
Stator Reactance	0.106 pu
Rotor Resistance	0.007 pu
Rotor Reactance	0.120 pu
Mag. Branch Reactance	4 pu

TABLE V REAL AND REACTIVE PARTS, CASE-2

	P (kW)	Q (kvar)
IM1-G1	-660	327.205
IM2-G2	-660	335.64

TABLE VI COMPARISON OF RESULTS, CASE-2

	NEW METHOD		PUBLISHED	
	IM1	IM2	IM1	IM2
slip	-0.00752	-0.00912	-0.00751	-0.00912
I_1 (A)	871.369	953.020	871.371	953.413
I_2 (A)`	21.067	21.597	21.2034	21.9022

TABLE VII VALIDATION OF LOAD-FLOW SOLUTION AT SELECTED BUSES, CASE-2

	NEW METHOD		PUBLISHED	
BUS	Magnitude (V)	Angle (deg.)	Magnitude (V)	Angle (deg.)
'808C'	14.95752	120.4485	14.959	120.4
'826B'	14.63782	-119.234	14.633	-119.2
'840B'	14.80022	-118.044	14.791	-118
'840C'	14.79969	122.5179	14.806	122.5
'848A'	14.79173	3.415665	14.806	3.4
'848B'	14.82455	-118.014	14.816	-118
'848C'	14.82893	122.5423	14.836	122.5
'850A'	14.62576	1.288783	14.632	1.3
'858A'	14.78789	3.344159	14.802	3.4
'858B'	14.83323	-118.044	14.824	-118
'858C'	14.82258	122.5381	14.829	122.5
'890B'	2.274698	-110.137	2.2743	-110.1
'G2B'	0.257733	-106.937	0.25769	-106.9

C. Case 3: Initialization of Induction Machine for Time-Domain Simulation

The objective of this case is to demonstrate how load-flow solution can be used to directly initialize the time-domain counterpart of IMs for transient studies.

The load flow analysis is used to evaluate and pass the slip of IM to its time domain counterpart. This is the only variable coming from the load flow solution (among phase voltages, powers and slip) and used by the time domain counterpart of IM.

The proposed initialization approach uses the proposed load flow solution in which the slip is a variable and there is only one real power or torque constraint. Fixed point methodology can also be used at the expense of large number of iterations, as discussed above.

As an alternative to the proposed initialization approach, it is also possible in EMTP [19] to specify an IM in the load-flow analysis as a PQ device with the nominal PQ parameters being the constraints (by fixing Q). In this case, the slip of the IM is computed at the end of the load flow analysis to initialize the time-domain counterpart. The computation is performed by using the equivalent circuit, voltage solution and electrical input power of the IM. This approach, which will be tagged as the "existing initialization method", cannot maintain seamless transition between load flow and time domain. The inaccuracy is due to the fixing of Q in load-flow, which normally depends on the voltage and therefore should not be fixed. As a result, the time-domain solution of the machine will not be accurate.

Note that, the proposed and the existing initialization approaches differ in the way the slip is evaluated using load flow.

Consider again the 4-BUS system of Fig. 2, but now with a balanced line and balanced 3-phase load, to focus on the initialization of the IM:

Line R positive sequence: 0.9 Ω
Line X positive sequence: 2.0 Ω
Line C positive sequence: 10^{-5} S
Load at BUS2: 1500 kW + 490.03 kvar per phase

Using the proposed load-flow solution, the input electrical power of the IM is fixed to 1000 kW and the slip is evaluated as 0.76792763. The proposed initialization approach, i.e. use of the slip from the load-flow solution in which the slip of the IM is a load-flow variable and its reactive power is not fixed, allows flawless transition from load-flow to time-domain, as shown in Fig. 6. If the IM is initialized using the load-flow solution with specified PQ constraints, it cannot maintain these constraints in time-domain simulation as shown in Fig. 6 where the real power in time domain reaches up to 1090 kW and the reactive power reduces to 542 kvars.

Simulation results for the original unbalanced 4-BUS system of Fig. 2 are presented in Fig. 7 and Fig. 8. This again demonstrates the accuracy of the proposed load-flow solution for the time-domain initialization of unbalanced networks. It is noticed that the instantaneous power has a slight small variation at the beginning of the simulation, this is because the load-flow solution calculates and imposes average power, not instantaneous. The network is unbalanced and that is why the power now oscillates around its average. The average power in time domain is equal to 1000 kW as exactly specified in load-flow calculations when the proposed load-flow initialization is used. If the IM is initialized using the load-flow solution with specified PQ constraints, it cannot maintain these constraints in time-domain as seen in Fig. 7 and Fig. 8 where the real power in time domain goes down to 980 kW from 1000 kW and the reactive power goes down to 482 kvar from 663 kvar.

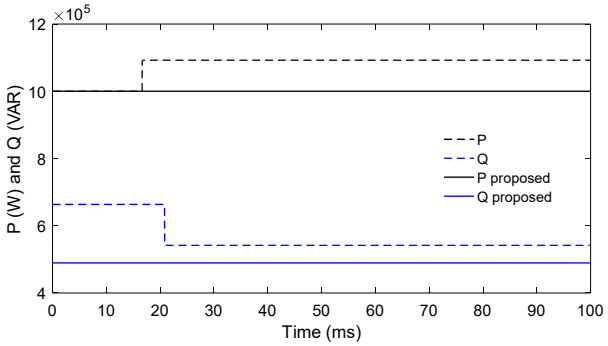

Fig. 6 PQ input of IM from load-flow to time-domain, dashed line starts with nominal PQ and is refreshed with actual PQ in time-domain, the solid line starts with proposed new load-flow solution (Q not fixed) and is refreshed with actual PQ in time-domain, Case-3

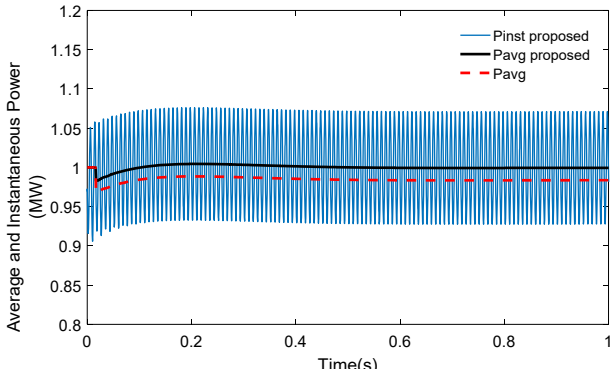

Fig. 7 PQ input initialization of IM, unbalanced 4-BUS Case-1, instantaneous active and average active powers. Solid line is initialized with the New Method and refreshed with actual average P measurement in time domain. Dashed line starts with specified P (PQ constraint) and is refreshed with actual P in time-domain.

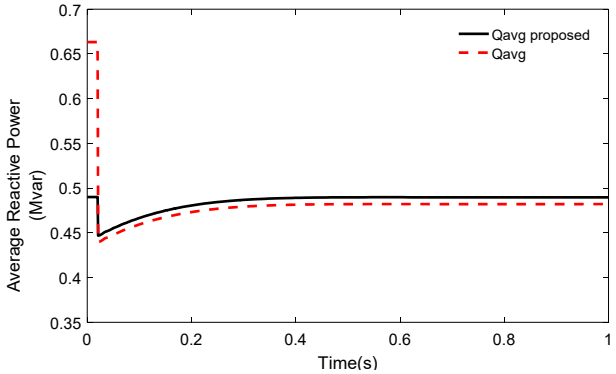

Fig. 8 PQ input initialization of IM, unbalanced 4-BUS Case-1, average reactive powers. Solid line is initialized with the New Method and refreshed with actual average Q measurement in time domain. Dashed line starts with specified Q (PQ constraint) and is refreshed with actual average Q in time-domain.

D. Case 4: Initialization from load-flow and detailed transient studies

Consider again the unbalanced IEEE 34-Bus Test Feeder with the two IMs of Fig. 4. At 300 ms a short circuit is triggered at BUS 888 on phase A. The short circuit is removed at 400 ms.

In Fig. 9, the initialized phase currents and following time-domain solutions of the IM named G1 is shown.

In [25], only the electrical output power of the generators is specified (which corresponds to the input electrical power of the IMs in this paper with a negative sign) but it is necessary to specify the reactive power constraint for the existing initialization method, and it is calculated as 161.1 kvars by imposing nominal voltage at the terminals of the machine and nominal input electrical power of -660 kW.

Fig. 10 compares the currents of phase c when the IM named G1 is initialized with the proposed approach and the existing initialization method. The peak current is evaluated as 28% less with the existing initialization method.

Fig. 11 and Fig. 12, show the electrical power inputs of the IMs G1 and G2 respectively obtained with different initialization methods. The oscillations in real power are due to the unbalanced network. As explained above, this is also the cause for the small startup variations in initial powers. When the average powers are considered, the achieved accuracy with the proposed initialization method is excellent for time-domain computations as the constraint of 660 kW in load-flow is maintained in time domain simulations as precisely as up to one decimal place.

If the IMs are initialized using the existing initialization method by fixing P and Q in load-flow (PQ constraint), then the average power is measured as -405 kW for G1 and -362 kW for G2. Another option is to model the IMs in load flow by using constant slip considering nominal conditions. The IM in this case becomes a constant impedance component in the load-flow analysis, and the slip, computed as -0.00756 under 1 pu of voltage and nominal P conditions, is passed to the time domain counterpart without modification. In that case, the average powers in time domain are -662 kW for G1 and -564 kW for G2. Using constant slip provides better results than the existing initialization method from fixed PQ solution. The real power for G1 is almost equal to the real power constraint but still the difference is significant for G2. The better performance for G1 is explained with the fact that the load-flow solution with constant slips results in almost nominal positive sequence voltage at the terminals of G1 (1.02 pu) which is not the case for G2 (0.94 pu).

E. Computational Burden

For each IM, one additional row of equations is introduced in the system of equations given by (5) when the slip is considered as a load-flow variable. The additional number of non-zero terms in the Jacobian matrix of (5) is 13. It is not possible to measure its burden on solution time in small systems. To see the impact on the solution time including the complete LU factorization of the Jacobian matrix in (5), a larger system is required.

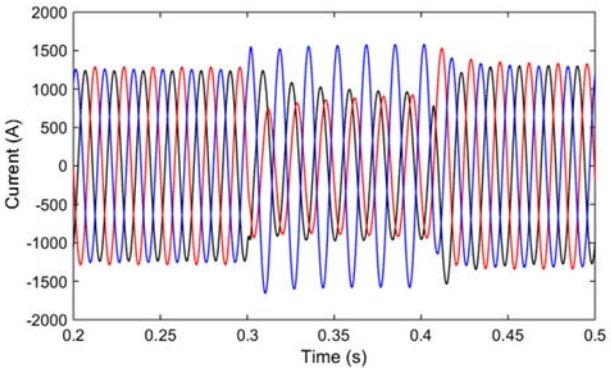

Fig. 9 IM-G1 currents, phases A, B and C, Case-4

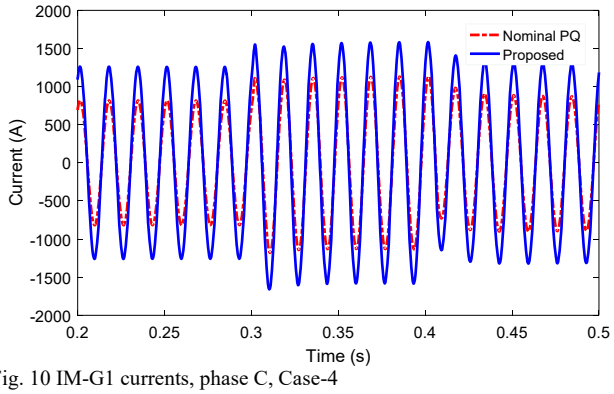

Fig. 10 IM-G1 currents, phase C, Case-4

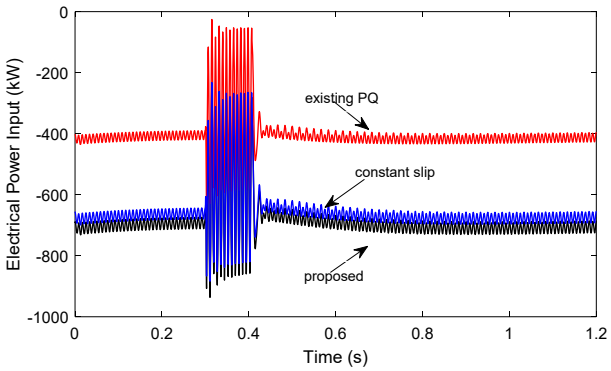

Fig. 11 Electrical instantaneous power input of G1, Case-4

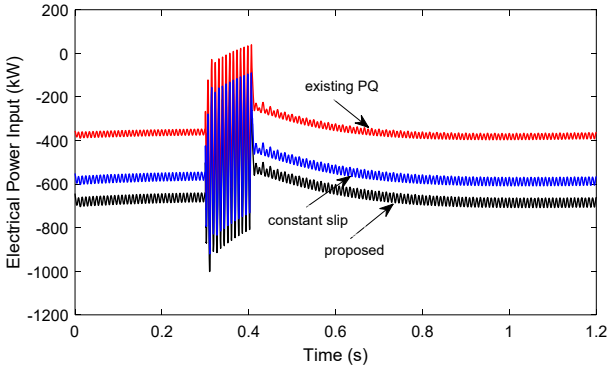

Fig. 12 Electrical instantaneous power input of G2, Case-4

The following timing results are based on MATLAB codes.

For timing purposes, the IEEE 8500-node test feeder described in [26] is taken here as the base case and 100 IM generators, 45 kW each, are arbitrarily connected to the network through additional transformers. The load-flow solution is reached in 3 iterations with the proposed new method. The average total time required for the solution of (5) increases to 113.17 ms from 99.75 ms (without IMs) resulting in an additional burden of 13.42 ms per iteration for solving the sparse system (5). If the IMs are directly connected to the network without transformers, then the additional burden per iteration reduces to 1.68 ms.

When the slips of the IMs are evaluated using an external procedure coupled to the load flow solver, i.e., using the power constraints and updated terminal voltages of the IMs after each load-flow iteration, as proposed in the existing literature, approximately 210 ms of computing time is required using a nonlinear equation solver. Only the equivalent circuit of the IM is used in the load flow formulation and it is updated at each iteration using the slip calculated by the external procedure. The timing given here is just to compute the slips of IMs with the external procedure after each load flow iteration. About 260 ms of solution time is needed using the iterative search method of [7] for the same purpose. If the iterative search algorithm is initialized using the slip value from the previous load-flow iteration, then the solution time reduces to approximately 60 ms. These solution times are per load-flow iteration and only for the evaluation of IM slips using an external procedure. Note that, the number of load-flow iterations required with fixed point methodology is 24 for the test case of interest. Therefore, the complete load flow requires at least 1.64 seconds of time for the evaluation of IM slips in addition to the time required for the 24-iterations of fixed-point load flow solution itself. The performance of the load flow solution depends on the specific method used and numerical procedures as discussed in [6]. The proposed new load flow method, on the other hand, requires only 3 iterations and 340 ms of total solution time for solving (5) three times. The solution of (5) provides the complete solution including IM slips.

Although it might be possible to optimize the external procedures for further gains in the computation of IM slips, it is important to underline that the proposed new method converges faster, is robust and the burden on solution time due to the addition of IMs is not perceptible for users.

VI. Conclusion

This paper contributes a new approach for the computation of unbalanced network load-flow solutions with the inclusion of induction machines. The load-flow solution formulation is based on modified-augmented-nodal analysis. Within this Newton solution method of nonlinear load-flow equations, the induction machines can be specified with electrical power input, mechanical power output or mechanical torque.

The proposed new approach is robust, can be applied to arbitrary networks without limitations and its Jacobian matrix based formulation is straightforward.

The proposed load-flow solution has been validated with published benchmarks. It has been demonstrated that for the 4-BUS test system the new method is capable of converging with only 3 iterations, whereas the published fixed-point approach uses 21 iterations. In the 34-BUS benchmark case, the new method requires only 4 iterations and the published fixed-point solution uses 28 iterations.

In addition to contributing to the unbalanced load-flow solution of induction machines, this paper demonstrates that the load-flow solution can be used to directly initialize its time-domain counterpart for the simulation of electromagnetic transients. The accuracy of time-domain initialization is a powerful approach for validating load-flow solutions. There is a seamless transition between load-flow and time-domain solutions when average IM powers are considered.

VII. References

[1] D. R. R. Penido, L. R. Araujo, S. Carneiro Junior, J. L. R. Pereira and P. A. N. Garcia, “Three-phase Power Flow Based on Four-Conductor Current Injection Method for Unbalanced Distribution Networks”, *IEEE Transactions on Power Systems*, vol. 23, pp. 494 - 503, 2008.

[2] D. R. R. Penido, L. R. Araujo, S. Carneiro Junior and J. L. R. Pereira, “A new tool for multiphase electrical systems analysis based on current injection method,” *Electrical Power and Energy Systems*, vol. 44, pp. 410–420, 2013.

[3] H. E. Farag, E. F. El-Saadany, R. El-Shatshat, and A. Zidan, “A generalized power flow analysis for distribution systems with high penetration of distributed generation,” *Elect. Power Syst. Res.*, vol. 81, no. 7, pp. 1499–1506, Jul. 2011.

[4] M. Z. Kamh, R. Iravani, "A Unified Three-Phase Power-Flow Analysis Model For Electronically Coupled Distributed Energy Resources," *IEEE Transactions on Power Delivery*, vol. 26, no. 2, pp. 899-909, 2011.

[5] M. Z. Kamh, R. Iravani, "Unbalanced Model and Power-Flow Analysis of Microgrids and Active Distribution Systems," *IEEE Transactions on Power Delivery*, vol. 25, no. 4, pp. 2851-2858, 2010.

[6] I. Kocar, J. Mahseredjian, U. Karaagac, G. Soykan, O. Saad, "Multiphase Load-Flow Solution for Large Scale Distribution Systems using MANA", *IEEE Transactions on Power Delivery*, vol. 29, no. 2, 2014, pp. 908-915.
[7] W. H. Kersting, J. S. Rathbun, "The analysis of an ungrounded Wye-Delta transformer bank serving an induction motor and single-phase lighting loads," *IEEE Transactions on Industry Applications*, vol. 36, no. 1, pp. 39-45, Jan/Feb 2000.
[8] R. C. Dugan, Induction Machine Modeling for Distribution System Analysis – Test Case Description, 2005/2006 *IEEE/PES Transmission and Distribution Conference & Exposition*, vols 1-3, pp 578-582.
[9] W. H. Kersting and W. Carr, "Induction machine phase frame model," in Proceedings of the 2005/2006 IEEE-PES Transmission and Distribution Conference and Exposition, Dallas, TX, USA, 2006, pp. 568 – 574.
[10] G.R. Cespedes, "New method for the analysis of distribution networks," *IEEE Trans. on Power Delivery*, vol. 5, no: 1, pp. 391-396, January 1990.
[11] C.S. Cheng and D. Shirmohammadi, "A three phase power flow method for real time distribution system analysis," *IEEE Trans. on Power Systems*, vol. 10, no. 2, pp. 671–679, May 1995.
[12] Y. Zhu and K. Tomsovic, "Adaptive power flow method for distribution systems with dispersed generation," *IEEE Trans. on Power Delivery*, vol. 17, no. 3, pp. 822–827, July 2002.
[13] R.M. Ciric, A. Padilha Feltrin, and L.F. Ochoa, "Power flow in four wire distribution networks – General approach," *IEEE Trans. on Power Systems*, vol. 18, no. 4, pp. 1283-1290, November 2003.
[14] G.W. Chang, S.Y. Chu, and H.L. Wang, "An improved backward/forward sweep load flow algorithm for radial distribution systems," *IEEE Trans. on Power Systems*, vol. 22, no. 2, pp. 882-884, May 2007.
[15] D. Shirmohammadi, H.W. Hong, A. Semlyen, and G.X. Luo, "A compensation based power flow method for weakly meshed distribution networks," *IEEE Trans. on Power Systems*, vol. 3, no. 2, pp. 753-762, May 1988.
[16] G.X. Luo and A. Semlyen, "Efficient load flow for large weakly meshed networks," *IEEE Trans. on Power Systems*, vol. 5, no. 4, pp. 1309-1316, November 1990.
[17] M. Dilek, F. de León, R. Broadwater, and S. Lee, "A Robust Multi-phase Power Flow for General Distribution Networks," *IEEE Trans. Power Systems*, vol. 25, no. 2, pp. 760-768, May 2010.
[18] W. H. Kersting, Distribution System Modeling and Analysis. Boca Raton, FL: CRC Press, 2002.
[19] J. Mahseredjian, S. Dennetière, L. Dubé, B. Khodabakhchian, and L. Gérin-Lajoie, "On a new approach for the simulation of transients in power systems," *Elect. Power Syst. Res*., vol. 77, no. 11, pp. 1514–1520, Sep. 2007.
[20] J. Mahseredjian: "Simulation des transitoires électromagnétiques dans les réseaux électriques", Édition 'Les Techniques de l'Ingénieur', Dossier D4130, February 2008.
[21] I. Kocar, J. S. Lacroix, F. Therrien, "General and simplified computation of fault flow and contribution of distributed sources in unbalanced distribution networks", *IEEE Power & Energy Society General Meeting*, 2012, pp. 1-8.
[22] F. Therrien, I. Kocar, and J. Jatskevich, "A Unified Distribution System State Estimator using the Concept of Augmented Matrices," *IEEE Transactions on Power Systems*, vol. 28, no. 3, pp. 3390-3400, 2013.
[23] http://ewh.ieee.org/soc/pes/dsacom/testfeeders/index.html
[24] J. Mahseredjian, S. Dennetière, B. Khodabakhchian and A. Xémard, "Induction machine modeling for distribution system analysis using initialization and time domain methods, " *IEEE Power & Energy Society General Meeting,* 2006, pp. 588-591.
[25] R. C. Dugan and W. H. Kersting, "Induction machine test case for the 34-bus test feeder-description," in Proc. *IEEE Power Eng. Soc. General Meeting*, Montreal, QC, Canada, June 2006.
[26] R. F. Arritt, and R. C. Dugan, "The IEEE 8500-node test feeder," Transmission and Distribution Conference and Exposition, 2010 IEEE PES, 19-22 April 2010.

Ilhan Kocar (SM'13) received the Ph.D. degree in electrical engineering from Polytechnique Montréal (affiliated with Université de Montréal), QC, Canada in 2009.

He worked as a Project Engineer at Aselsan Electronics Inc. (1998-2004) and as an R&D Engineer at CYME International T&D (2009-2011). He joined the faculty at Polytechnique Montreal in 2011. His research is on the development of concepts, models and methods for power systems analysis and simulation.

Ulas Karaagac (M'08) received the B.Sc. and M.Sc. degrees in electrical and electronics engineering from Middle East Technical University, Ankara, Turkey in 1999 and 2002, respectively, and the Ph.D. degree in electrical engineering from Polytechnique Montreal, Canada in 2011.

He was an R&D engineer at Information Technology and Electronics Research Institute (BILTEN) of the Scientific and Technical Research Council of Turkey (TUBITAK), from 1999 to 2007. He was a Ph.D. scholar at Polytechnique Montreal between 2007 and 2011, where he continued working as postdoctoral fellow and then as research associate until the end of 2016. He joined the Department of Electrical Engineering of Hong Kong Polytechnic University as Research Assistant Professor in December 2016. His research areas include modeling and simulation of large scale power systems.

Jean Mahseredjian (FM'13) received the Ph.D. degree from Polytechnique Montréal, Canada, in 1991. From 1987 to 2004, he was with IREQ (Hydro-Québec) working on research and development activities related to the simulation and analysis of electromagnetic transients. In December 2004, he joined the faculty of Electrical Engineering at Polytechnique Montréal.

Baki Cetindag received the B.Sc. degree in electrical and electronics engineering from Orta Dogu Teknik Universitesi, Ankara, Turkey in 2010. He is currently a Ph.D. student at Polytechnique Montréal, QC, Canada. His research interests are power system modeling, analysis and simulation.